Determination of thermal diffusivity for the correct design of iron castings

ROMANO BORCHIELLINI - Dipartimento di Energetica, Politecnico di Torino.
MICHELE CALÌ - Dipartimento di Ingegneria Meccanica, II Università di Roma, "Tor Vergata".
BRUNO DE BENEDETTI - Dipartimento di Scienza dei Materiali ed Ingegneria Chimica, Politecnico di Torino.
VALTER GIARETTO - Dipartimento di Energetica, Politecnico di Torino.
CARLO ALBERTO GORIA - Teksid, Divisione Fonderie Ghisa.

Abstract

A fuller understanding of the thermophysical characteristics of cast iron has been rendered necessary by recent changes in the design and manufacture of mechanical components, especially those employed in the automotive industry.
Thermal diffusivity is of particular importance in this respect. Its determination by means of a transient thermal step method is described in this paper. A thermal step is induced in test specimens by their rapid transfer from one thermostated environment to another at a higher temperature. Temperatures are then taken during the transient step at a point with known coordinates.
Simulation of this transient under different heat exchange conditions with a finite elements model (FEM), which can handle specimens of varying geometry, gives a grid formed of points representing Biot and Fourier numbers, and temperature values θ standardised within the range zero to one.
Thermal diffusivity is determined by taking the Biot and Fourier numbers that minimise the difference between the θ values observed experimentally and those on the curve supplied by the model. This parameter is then correlated with the metallurgical characteristics.

Riassunto

L'evoluzione progettuale dei componenti meccanici, specie quelli d'impiego automobilistico, ha reso necessaria una migliore conoscenza delle caratteristiche termofisiche delle ghise.
La diffusività termica è di particolare importanza, talché si propone un metodo di misura in transitorio, tramite un impulso a gradino, di facile esecuzione. I provini sono infatti sottoposti ad un transitorio termico tramite il rapido passaggio da un termostato ad un altro a temperatura più alta, registrando la variazione di temperatura in un punto prefissato del campione.
La simulazione di transitori in condizioni di scambio termico variabile viene preventivamente eseguita tramite un modello ad elementi finiti (FEM), che può valutarli per geometrie variabili dei provini. Il calcolo fornisce una griglia di numeri di Biot e Fourier al variare della temperatura θ normalizzata tra zero ed uno. La diffusività termica è determinata trovando i numeri di Biot e Fourier che rendono minima la differenza tra i valori di θ sperimentali e quelli forniti dal modello. Infine viene correlata la diffusività termica con le caratteristiche microstrutturali delle ghise esaminate.

Introduction

Evaluation of the thermophysical properties of materials is of major importance in many engineering applications. In the case of thermal diffusivity, the techniques proposed so far suffer from two drawbacks in that they require the use of complex instrumentation and specifically prepared test specimens (following an investigation of these difficulties). An alternative method elaborated at the Department of Energetics of the Turin Polytechnic was subsequently validated on samples of Armco iron, which is used as the reference standard on account of the abundant data on its properties to be found in the literature (2).

The method used to process the experimental data now being perfected (3), it was thus decided to extend the application of the technique to metal alloys, such as cast iron. This class of materials, indeed, is of particular interest, since its thermophysical properties are very closely dependent on their microstructure.

Despite the tendency to resort to lighter materials, cast iron has continued to hold pride of place in the automotive industry, especially on account of its suitability for the production of heavy-duty components with complex geometries. Particular importance is also attached to those of its physical and mechanical characteristics that have the most direct influence on the thermal behaviour of the castings used, for example, to make engine blocks, cylinder heads, exhaust manifolds, brake drums and discs, etc.

This paper is a contribution towards the evaluation of the thermophysical characteristics of cast iron. A set of sufficiently reliable thermal diffusivity values obtained with a simple, fast measurement method is presented.

Diffusivity measurement method

The main points upon which the method is based will now be described. A more detailed account will be found in the paper already referred to (3).

The phenomenon to be examined is heat transmission energy by conduction in a continuous body of known shape, subjected to a step pulse provoked by the virtually instantaneous passage from a thermostat at a certain temperature to another at a higher temperature.

The operation consists of the following stages:
i) The finite elements method is used to calculate (for the geometrical configuration of the body being studied) as many heat transients as the number of Biot numbers considered. The temperature is dimensionless and hences varies between 0 and 1.

ii) Calculation of the finite elements gives a series of points lying on the surface $\theta_c = \theta_c(\beta, \tau)$, where β and τ are the Biot and Fourier numbers respectively. From the definition of τ, the surface can be expressed as $\theta_c = \theta_c(t; \beta, \alpha)$, where α is the thermal diffusivity and t is the generic time instant of the transient. The appearance of the calculated surface is illustrated in Fig. 1.

iii) Experimentation gives a curve θ_s in function of time. An iterative method is used to find the α and β values providing the minimum discrepancy between θ_c and θ_s.

Experimental part

The measurements were made on cast-iron cylindrical test specimens. A ∅ 2 mm axial hole was used to insert a chromel-alumel thermocouple in their geometrical centre by brazing its joint in this position with a silver alloy, and insulating the rest of it from the walls of the hole with a polymer sheath. The hole was then filled with a cold-polymerising glue.

The layout of the experimental apparatus can be seen in Fig. 2. The thermocouple signals were acquired by a digital voltmeter controlled by a computer, which stored the readings on its hard disk.

The experimental apparatus was lastly completed with thermostats at T1 = 0°C and T2 = 70°C respectively. The rapid passage of the specimen from the first thermostat to the second permitted attainment of the "step" desired of the temperature of the environment in which this was immersed.

The cylindrical specimens had turned sides and a ground base (machining tolerance: ±0.01 mm). Their ∅ was 44 mm and their length ranged from 14.22 to 43.58 mm. The nature and composition of the cast iron are shown in Table 1. Eight transients were measured for each specimen.

Table 1 - Characteristics of the cast irons examined

Sample	Components										Hardness
	C	Si	Mn	Ni	Cr	Mo	S	Cu	Sn	Mg	HB
GGL 1	3.38	2.10	1.06	0.22	0.25	0.21	.090	0.20	.060	—	223
GGL 2	3.68	2.10	0.64	0.06	0.19	0.01	.100	0.32	.019	—	149
GGL 3	3.36	2.41	0.57	0.06	0.12	0.01	.120	0.92	.016	—	199
GGS 4	3.67	2.78	0.22	0.03	0.03	tr.	.009	0.23	.008	—	207
GGV 5	3.67	2.11	0.19	0.03	0.03	tr.	.007	0.74	.008	.022	229

Experimental results

The time/temperature curves of time at the geometric centre of the tallest test specimens are shown in Fig. 3. These curves were obtained by performing a least squares regression on all the points measured in the set of tests for each type of cast iron.

The distinct differences in behaviour are closely linked to the morphology of the graphite in the

Table 2 - Thermal diffusivity of the cast irons examined

Sample	Type of graphite	Pearlite (%)	Mean flake length (mm)	Diffusivity (m^2/s)
GGL 1	I A 4	100	0.14	$0.2193 \cdot 10^{-4}$
GGL 2	I A 3	100	0.25	$0.2455 \cdot 10^{-4}$
	I A 5		0.12	
GGL 3	I A 3	100	0.27	$0.1594 \cdot 10^{-4}$
GGS 4	VI A	60	—	$0.1094 \cdot 10^{-4}$
GGV 5		60	—	$0.1731 \cdot 10^{-4}$

matrix, and to a lesser extent to the nature of the matrix itself and the presence of particular alloy elements.

Table 2 shows that the thermal diffusivity of nodular graphite iron is relatively slight, whereas that of flaked graphite iron is significantly higher. Similar results can be found in the literature (4-7), though no explanation for this difference has been advanced.

Cast iron can be described as a composite material in which graphite is the component with the highest degree of thermal conductivity. This latter phase is also known (8) to display marked anisotropy that corresponds to the flow direction with respect to the basic reticular plane, and is more or less enhanced by the origin of the graphite. For all these reasons, therefore, the contribution of this phase to conduction phenomena will depend on whether it is in the form of flakes, nodules or spheroids. Graphite thus acts as a thermal bridge within the matrix, and the value of the contact resistance between the phases is decisive. In the case in point, the matrix-graphite contact may differ on account of solidification of the alloy starting from the molten form, as well as the effect of the magnesium-type nodularising elements.

Various theories have been advanced with regard to the nucleation and growth of nodular graphite (9,10). Discussion of their merits lies outside the scope of this paper. It may none the less be pointed out that the reduced thermal diffusivity observed for nodular iron fits in well with the view that nucleation takes place in the presence of gas bubbles, with growth of the spheroid through filling of the cavity with a centripetally developing lamella wrapped around itself. Comparison of the three types of flaked cast iron examined revealed marked differences in behaviour. Application of the usual specific heat and density values to the first two specimens of Table 2 gave a thermal conductivity of about 80 W/[m.K], which is well above that reported in the literature, whereas the value for specimen 3 was fully in line with the published data. Since there were no very significant differences between iron 1 and iron 3, the only possible explanation is that the contribution of graphite to heat conduction varies considerably in function of the higher or lower matrix-graphite contact resistance established on solidification. The appreciably greater diffusivity of specimen 2 compared with specimen 1, on the other hand, can be attributed to its higher carbon content.

The thermal diffusivity values of the "compact" graphite irons were surprisingly different from those in the literature. Here the graphite could perhaps be seen as the term marking the transition from nodules to flakes, and the diffusivity values for this class of materials should lie between those of the other two. In this respect, the diffusivity measured for specimen 5 would be regarded as partly out of line with the usual values in the literature (7).

This was an iron obtained by using the "in-mould" spheroidising process (11), with a Fe-Si-Mg solution factor producing a reduced effect and hence only partial spheroidisation. Microscopic examination showed that the graphite was partly spheroidal and partly vermicular, while its content varied greatly from one zone to another. Very different thermal diffusivity values, in fact, were measured in two specimens taken from opposite parts of the same bar. The higher value was obviously found for the specimen that more closely resembled a flaked graphite, whereas the lower value ($\alpha = 0.1132.10^{-4}$) came from a specimen with a height of 14.22 mm, and hence a greater degree of uncertainty — a point dealt with in greater detail below. This value could be taken as representative of a typical nodular iron microstructure.

In addition to the effect of the graphite, a certain importance should also be assigned to the type of metal matrix, since it is well known that the conducutivity of ferrite is much higher than that of pearlite (12). In addition, when the graphite morphology and the type of matrix are the same, the effect of the alloy elements should be taken into account. It was found, however, that specific addition of copper to alloy 3 compared with alloy 1, which otherwise had practically the same composition, particularly with regard to carbon, resulted in a negligible difference in the thermal properties. It should also be pointed out that these two alloys have a very similar microstructure (almost totally pearlitic), even though the mean dimension of their flakes is slightly different. The conclusion to be drawn is that the matrix-graphite contact resistance is the characteristic of an alloy that has the greatest influence on its thermal diffusivity, since it can either appreciably improve its conduction compared with the matrix, or, as in the case of nodular iron, reduce it because the nodule cavities act as insulating gaps in the continuity of the matrix.

These heat conduction phenomena can be illustrated by analogy with the electrical type of circuit diagram shown in Fig. 4, where an increase in the matrix-graphite contact resistance (R_c) means that the flow is almost entirely shunted through the matrix (R_m). When R_c is negligible, on the other hand, the contribution made by the graphite to conduction (R_g) will be greater the higher its volumetric fraction, and the better its orientation and arrangement in the matrix, in view of its already mentioned thermal anisotropicity.

Reliability of the results

The thermal diffusivity values shown in Table 2 were obtained from experimental patterns following the use of regression to eliminate the signal background noise picked up by the acquisition system. These values are the means for the 8 tests performed on each cast iron specimen. The uncertainty associated with each mean and its per cent value are indicated in Table 3.

Table 3 - Confidence intervals of the results

Sample	Diffusivity (m^2/s)	Confidence interval (%)
GGL 1	$(0.2193 \pm 0.0135) \cdot 10^{-4}$	± 6.1
GGL 2	$(0.2455 \pm 0.0089) \cdot 10^{-4}$	± 3.6
GGL 3	$(0.1594 \pm 0.0036) \cdot 10^{-4}$	± 2.3
GGS 4	$(0.1094 \pm 0.0023) \cdot 10^{-4}$	± 2.1
GGV 5	$(0.1731 \pm 0.0051) \cdot 10^{-4}$	± 3.0

The small-samples theory (13) was used to determine uncertanty to 95% significance. The sample has seven degrees of freedom ($g = N - 1$). In the event of reiteration of a set of measurements, the confidence interval thus defined ensures that within these limits the diffusivity value will again be found in 95% of cases.

The reason why the interval is more or less extensive around the mean lies in errors associated with the experimental procedure and the instruments employed, together with errors stemming from the insufficiency of the model as a perfect description of the real phenomenon (3). Among the first class of errors, mention must be made — on account of their relative importance — of fluctuations in the thermostat temperature, due to accidental circumstances with an incidence varying from one test to another, and uncertainty in the precise determination of the origin of the time base.

In addition to the errors described above, which are associated with the execution of the experiments, consideration must also be given to that arising from uncertainty in the exact measurement of the specimen dimensions, the temperature measurements, and the position of the thermocouple inside the specimen. In the case in point, owing to the accuracy of the size measurements and the positioning of the thermocouple, this error tends to cancel itself out, whereas the stated temperature error ($\pm 0.05°C$) means that a further $\pm 1.5\%$ uncertainty must be added to the diffusivity values (3).

The five tests were repeated with shorter specimens ($h = 14.22$ mm) of irons 2 and 4 to obtain a better idea of the reliability of the experimental apparatus. The values in this case $0.2487.10^{-4}$ and $0.1189.10^{-4}$ respectively, were close to those for the longer specimens, though the confidence intervals were distinctly greater, namely $\pm 31.2\%$ and $\pm 27.4\%$ with respect to the mean. It is clear that in this case the errors associated with the type of apparatus have a greater influence on heat transfer. Indetermination of the initial instant, for example, may even be responsible for errors of as much as $\pm 20\%$ (3).

Conclusions

Our results demonstrate the soundness of the method proposed, since it proved possible to determine the thermophysical characteristics of metal alloys, such as thermal diffusivity for example, with techniques not dependent on the geometry of the specimen material.

Measurements taken from specimens differing in size revealed the difficulties involved in the correct acquisition of the transient when a specimen has a relatively small thermal capacity, because the experimental equipment was not fast enough to follow the development of the phenomenon. On the other hand, despite the very simple nature of the apparatus, the results obtained from specimens with a greater thermal capacity can be regarded as acceptable in virtue of the confidence interval given for them by Student's test.

It should be noted that some values were not on line with those given in the literature. These discrepancies, however, can be explained in microstructural terms. It was found, in fact, that the contact resistance between the graphite and the metal matrix has a preponderant influence in thermal diffusivity. Were this influence to be left out of account, it would be impossible to find a reason for the relatively modest diffusivity of nodular as opposed to flaked cast iron. Furthermore, the differences observed between two flaked irons that were similar in composition and in the type of their metal matrix can be explained by supposing that their graphite did not make the same contribution to the transmission of heat.

References

[1] Borchiellini R., Calì M., De Benedetti B., Giaretto V., Ruscica G. *Un metodo rapido per la misura della diffusività termica di materiali metallici*, Atti del 6° Congresso Nazionale sulla Trasmissione del Calore (UIT), Bari 9 - 11 Giugno 1988, pp. 467, 479.

[2] Touloukian Y. S., *Retrieval Guide to Thermophisical Properties Research Literature*, New York - Mc. Graw Hill 1960-1963.

[3] Borchiellini R., Calì M., De Benedetti B., Giaretto V. *Sulla determinazione sperimentale della diffusività termica dei materiali metallici con un metodo impulsivo a "gradino"*, Pubblicazione interna Dipartimento di Energetica Politecnico di Torino, PT DE/FT 159, Novembre 1988.

[4] Hoyt S. L. *Metals and Alloys Data Book*, Reinhold Publishing Corporation, New York 1943, p. 193.

[5] Sinnott M. J. *Thermal Conductivity of Nodular Iron* Transactions Aime, p. 1016, Journal of Metals, August 1953.

[6] Plessers J., Lietaert F., Van Eeghem J. *Determination rapide du degré de nodularité d'une fonte traitée au magnésium*, Fonderie 389, Mai 1979, pp. 159-167.

[7] Appendino P., Montorsi M. *Ghise con grafite vermiculare*, Meccanica Pratica n. 1, 1984, pp. 62-65.

[8] Pascal P. *Nouveau Traité de Chimie Minérale*, Tome VIII, Parigi 1968, Masson et C., pp. 275-280.

[9] Appendino P., Montorsi M. *Nucleazione della grafite nella ghisa sferoidale*, La fonderia italiana n. 3, 1979, pp. 57-67.

[10] Appendino P., Montorsi M. *Crescita della grafite nella ghisa sferoidale*, La fonderia italiana n. 7/8, 1979, pp. 3-13.

[11] Remondino M., Pilastro F., Natale E., Costa P., Peretti G., *Inoculation and Spheroidizing Treatments directly inside the Mold*, Transaction of the American Foundryments Society, 1974, Vol. 82, pp. 239-252.

[12] Metals Handbook Vol. 1 *Properties and selection of metals*, p. 393, American Society for Metals, Ohio 1961.

[13] Guttman I., Wilks S.S., Stuart Hunter J. *Introductory engineering statistics* John Wiley & Sons, New York, 1971.

Figure captions

Fig. 1: X = normalised temperature; Y = Biot's number; Z = Fourier's number.

Fig. 2: Layout of the experimental apparatus.

Fig. 3: Temperature curves in the centre of the test specimens.

Fig. 4: Circuit diagram showing an electrical analogy for the transmission of heat in cast iron.

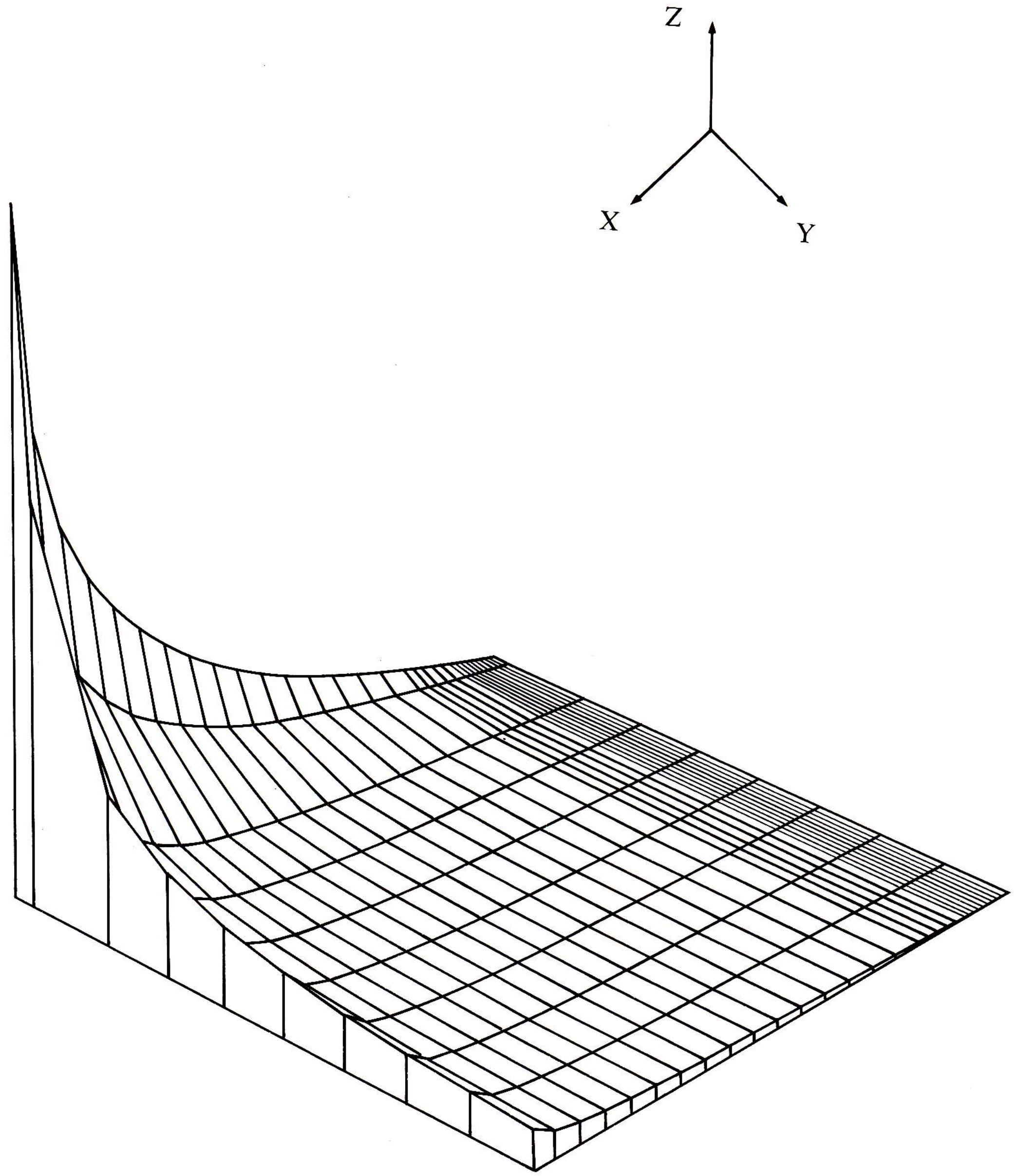
Z
X
Y

Fig. 1

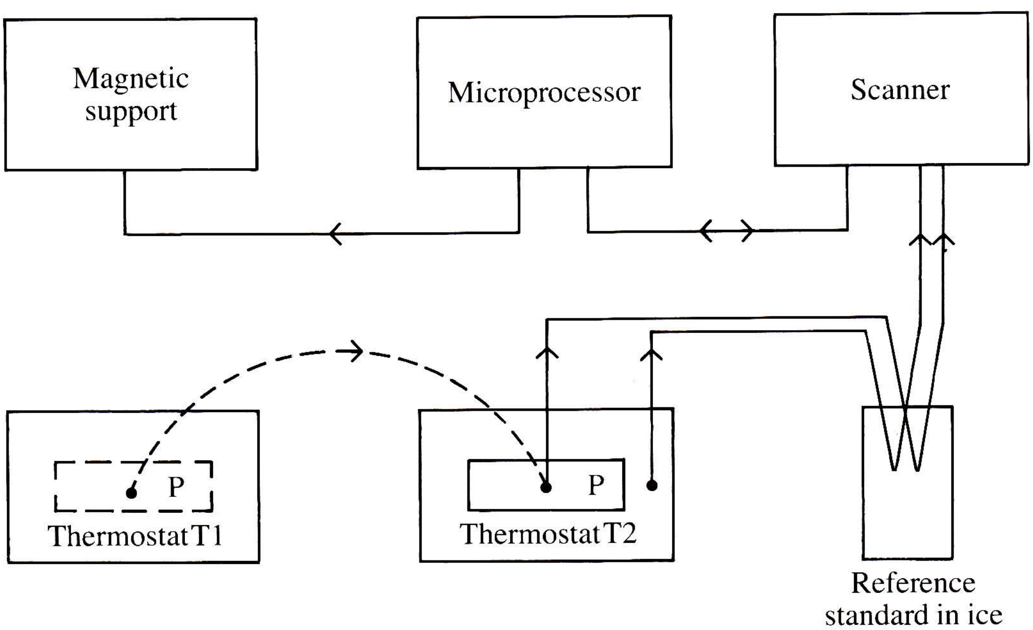
Magnetic support
Microprocessor
Scanner
P
Thermostat T1
P
Thermostat T2
Reference standard in ice

Fig. 2

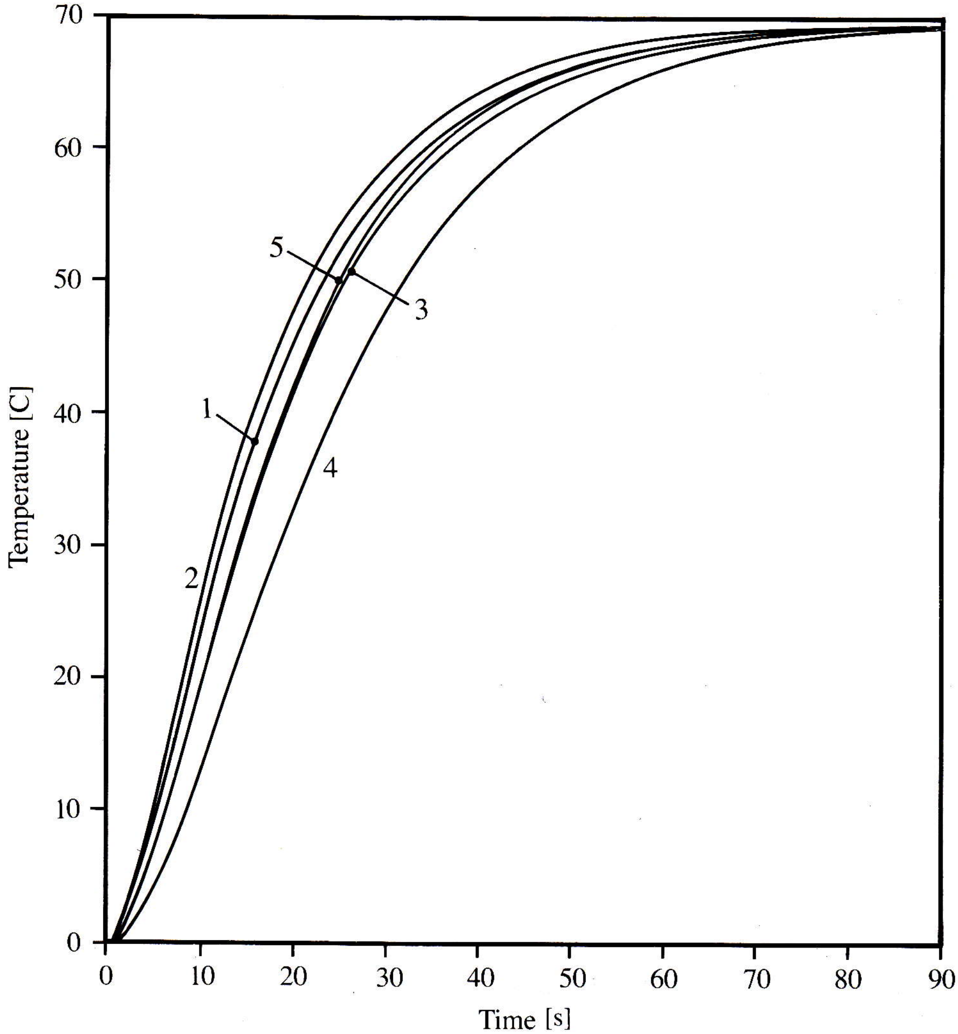

Fig. 3

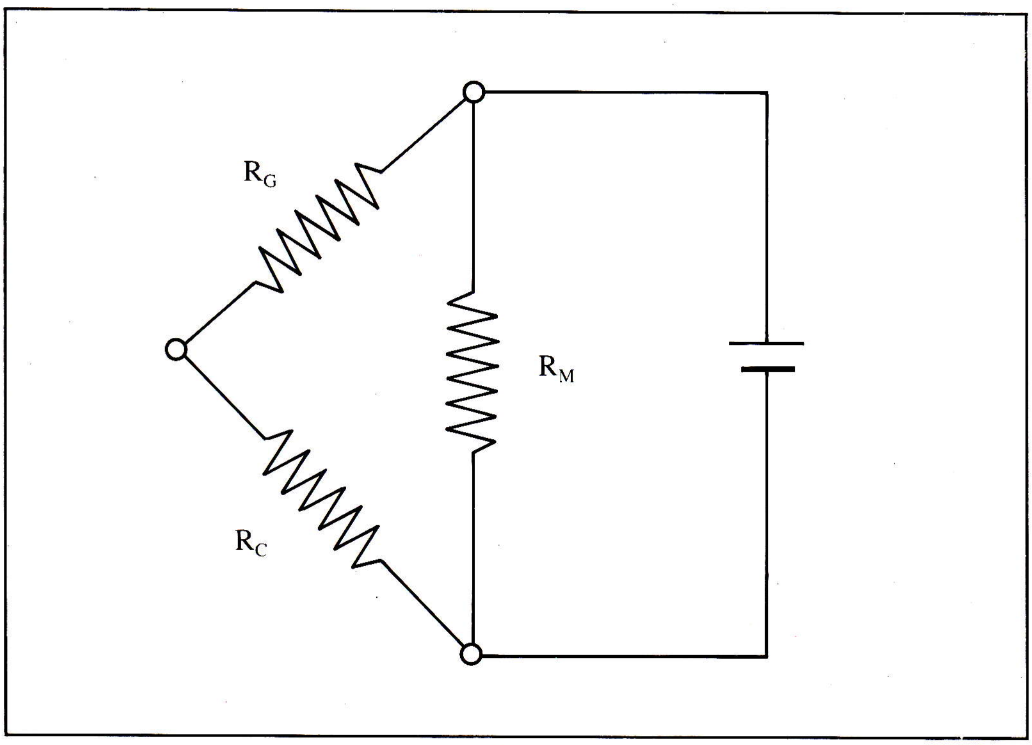

Fig. 4